Journal of Science and Technology in Civil Engineering, HUCE (NUCE), 2022, 16 (4): 10–29

INVESTIGATE THE BENDING AND FREE VIBRATION RESPONSES OF MULTI-DIRECTIONAL FUNCTIONALLY GRADED PLATES WITH VARIABLE THICKNESS BASED ON ISOGEOMETRIC ANALYSIS

Son Thai[a,b,*], Qui X. Lieu[a,b]

[a]*Department of Civil Engineering, Ho Chi Minh City University of Technology (HCMUT), 268 Ly Thuong Kiet Street, District 10, Ho Chi Minh City, Vietnam*
[b]*Vietnam National University Ho Chi Minh City, Linh Trung Ward, Thu Duc City, Ho Chi Minh City, Vietnam*

Article history:
Received 16/5/2022, Revised 16/6/2022, Accepted 23/6/2022

Abstract

This study investigates the static bending and free vibration behaviour of Multi-directional Functionally Graded (MFGM) plates having a variable thickness. With this regard, the third-order shear deformation plate theory is used to describe the kinematic relation. Material properties of MFGM are assumed to be graded in spatial direction within the plate's volume and the effective material properties are calculated based on the power-law approach. The governing equations are derived based on Hamilton's principle and the Isogeometric Analysis (IGA) is employed as a discretization tool to develop system equations. Several numerical examples are conducted to verify the accuracy of the proposed approach and investigate the influence of different geometrical and material parameters on the behaviour of MFGM plates.

Keywords: third-order shear deformation plate theory; multi-directional functionally graded materials; isogeometric analysis; linear analyses.

https://doi.org/10.31814/stce.nuce2022-16(4)-02

1. Introduction

In various fields of structural engineering, plate-like structures with variable thickness are broadly adopted due to their specific mechanical characteristics with the efficient use of materials [1–4]. Tapered plates, whose thickness is varied linearly in one or two directions, are widely considered as the most common type of variable thickness plates. Therefore, investigations on their mechanical behaviour have been extensively conducted by various researchers in the literature [5–12]. In addition, other types of variable thickness plates with nonlinear thickness variation have been investigated for practical application recently [13, 14], especially in the adoption of Functionally Graded Materials (FGMs) for such structures.

Developed by Japanese scientists in the late 80s of the last century, FGM [15] is broadly viewed as a novel artificial material. Categorized as a composite material, FGM is made from different material constituents, normally ceramic and metal. The development process allows the material properties to

*Corresponding author. *E-mail address:* son.thai@hcmut.edu.vn (Thai, S.)

change smoothly within the plate's domain, hence the adoption of FGM in practical structures can eliminate the common drawback of traditional laminated composite materials, such as the delamination, shear stress concentrations, etc. Thanks to their advanced features, a huge number of studies in the literature have been devoted to studying the mechanical properties and application of beams, plates, and shells made from FGMs [16]. Literature reviews [16–18] indicated that a large portion of the previous research focused on the analysis of uniform thickness structures, which are made from FGM with material constituents being graded in the thickness direction of the structures. While the research for FGM plates with variable thickness is still limited. Tran et al. [19] studied the static bending and free vibration behaviour of variable thickness FGM porous plates by using the edge-based smoothed finite element method. The static bending response of FGM plates with variable thickness was investigated by Phan [20] based on a new mixed four-node quadrilateral element. Other notable investigations on the bending and free vibration responses of FGM plates with variable thickness are Lal and Saini [21], Kumar et al. [22], Kumar et al. [23, 24], Minh et al. [25], and Hosseini-Hashemi et al. [26].

In recent studies on the applications of FGM for advanced structures subjected to severe loading conditions, it was found that the normal thickness-gradation FGMs are not efficient and the use of spatial variations of material constituents should be adopted for optimal design [27, 28]. Hence, various studies have been devoted to investigating the structural response of Multi-directional Functionally Graded Materials (MFGMs) recently. The bending and free-vibration of in-plane bi-directional FGM plates were analyzed by Lieu et al. [29, 30]. Alipour et al. [31] presented a study on the free vibration behaviour of variable thickness MFGM circular plates resting on elastic foundations. Shariyat and Alipour [32] proposed a power series solution to investigate the dynamic responses of viscoelastic MFGM variable thickness plates. Thai et al. [33] studied the bending of free vibration of MFGM plates in the thermal environment. Some other remarkable investigations on the bending and free vibration of MFGM plates with variable thickness are Temel and Noori [34], Zhong et al. [35], and Jalali and Heshmati [36].

In general, it is seen that the research on bending and free vibration MFGM plates is still restricted. Furthermore, the previous studies on MFGM mostly focus on the in-plane variation of constituent materials. Therefore, the main objective of this study is to investigate the bending and free vibration responses of MFGM plates with variable thickness, where the material constituents are spatially varied within the plates' domain. With this regard, the third-order shear deformation theory is employed to represent the kinematic relations. The governing equations are developed based on Hamilton's principle. The Isogeometric Analysis (IGA) approach is employed as a numerical method to solve the governing equation. Various numerical examples are conducted to validate the accuracy of the proposed approach. Parametric studies are also conducted to investigate the effects of geometrical and material parameters. The obtained results could be served as benchmark solutions for future investigations.

2. Theoretical formulations

2.1. Material properties of MFGM

In Fig. 1, the geometries of variable-thickness rectangular and circular MFGM plates and corresponding Cartesian coordinates are depicted. It is assumed that the rectangular plate has a variable thickness along one direction and the circular plate has a variable thickness in the radius direction. For rectangular plates, the side length in the x-direction is a and the side length in the y-direction

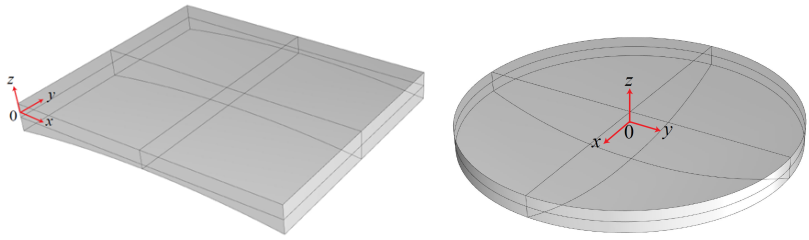

Figure 1. Geometries and Cartesian coordinates of variable thickness rectangular (the side length in the x-direction is a and the side length in the y-direction is b) and variable thickness circular plates having a radius of R

is b, the origin of the Cartesian coordinates system is located at a corner of the plates. For circular plates having radius R, the Cartesian coordinate system is located at the centre of the plate. By adopting the rule of mixture, material properties vary continuously within the plates' domain based on the following equations

$$P(x,y,z) = (P_c - P_m)\, V_c(x,y,z) + P_m \tag{1}$$

in which $P(x,y,z)$ denotes a generic material property, e.g. elastic modulus $E(x,y,z)$, Poisson's ratio $\nu(x,y,z)$, mass density $\rho(x,y,z)$. P_c and P_m represent the material properties of ceramic and metal components. $V_c(x,y,z)$ is the volume fraction of ceramic material and is represented by mathematical formulas of spatial coordinates.

2.2. *Third-order shear deformation plate theory of Reddy [37] and governing equations*

In this study, the third-order shear deformation plate theory proposed by Reddy [37] is used to describe the kinematic relations. The theory is widely considered to be the most reliable plate model to consider the influence of the shear deformation effect in thin and thick plates without considering the shear correction factor but remains condensed form. The spatial displacements at any point within a variable thickness plate are given as follows [37]

$$\begin{aligned} u_1 &= u + f(z)\,\theta_x - g(z)\,w_{,x} \\ u_2 &= v + f(z)\,\theta_y - g(z)\,w_{,y} \\ u_3 &= w \end{aligned} \tag{2}$$

where the comma notation denotes the partial derivative, u, v, and w are the translations of any point in the referenced plane (the plane where the Cartesian coordinate is located), θ_x and θ_y are the rotations of normals to mid-plane around the y- and x-axes, $f(z)$ and $g(z)$ are the functions defined as follows

$$f(z) = z - 4z^3/3h^2; \quad g(z) = 4z^3/3h^2 \tag{3}$$

$$h(x,y) = z_t(x,y) - z_b(x,y) \tag{4}$$

with $z_t(x,y)$ and $z_b(x,y)$ being the coordinates of the top surface and bottom surface, respectively.

Based on the theory of elasticity, the strains are defined as follows

$$\varepsilon_{xx} = u_{,x} + f(z)\,\theta_{x,x} - g(z)\,w_{,xx} \tag{5}$$

$$\varepsilon_{yy} = v_{,y} + f(z)\,\theta_{y,y} - g(z)\,w_{,yy} \tag{6}$$

$$\gamma_{xy} = u_{,y} + v_{,x} + f(z)\left(\theta_{x,y} + \theta_{y,x}\right) - 2g(z)\,w_{,xy} \tag{7}$$

$$\gamma_{xz} = f'(z)\,\theta_x + (1 - g'(z))\,w_{,x} \tag{8}$$

$$\gamma_{yz} = f'(z)\,\theta_y + (1 - g'(z))\,w_{,y} \tag{9}$$

The constitutive equation is given by

$$\begin{Bmatrix} \sigma_{xx} \\ \sigma_{yy} \\ \sigma_{xy} \\ \sigma_{xz} \\ \sigma_{yz} \end{Bmatrix} = \begin{bmatrix} Q_{11} & Q_{12} & 0 & 0 & 0 \\ Q_{21} & Q_{22} & 0 & 0 & 0 \\ 0 & 0 & Q_{44} & 0 & 0 \\ 0 & 0 & 0 & Q_{55} & 0 \\ 0 & 0 & 0 & 0 & Q_{66} \end{bmatrix} \begin{Bmatrix} \varepsilon_{xx} \\ \varepsilon_{yy} \\ \gamma_{xy} \\ \gamma_{xz} \\ \gamma_{yz} \end{Bmatrix} \tag{10}$$

where

$$Q_{11} = Q_{22} = \frac{E}{1-\nu^2}; \quad Q_{12} = Q_{21} = \frac{E\nu}{1-\nu^2}; \quad Q_{44} = Q_{55} = Q_{66} = \frac{E}{2(1+\nu)} \tag{11}$$

By using Hamilton's principle, the governing equations for static bending and free vibration problems are given as follows

- For static bending problems

$$\int_{\Omega} \delta\hat{\boldsymbol{\varepsilon}}^T \hat{\mathbf{D}}\hat{\boldsymbol{\varepsilon}} d\Omega = \int_{\Omega} q\delta w d\Omega \tag{12}$$

- For free-vibration problems

$$\int_{\Omega} \delta\hat{\boldsymbol{\varepsilon}}^T \hat{\mathbf{D}}\hat{\boldsymbol{\varepsilon}} d\Omega = \int_{\Omega} \ddot{\mathbf{u}}\mathbf{m}\delta\ddot{\mathbf{u}} d\Omega \tag{13}$$

where Ω denotes the domain of referenced plane and superscript dot notation represents the derivative with respect to time. Other components in Eqs. (12) and (13) are given as follows:

$$\hat{\boldsymbol{\varepsilon}} = \begin{Bmatrix} \boldsymbol{\varepsilon}_0 \\ \boldsymbol{\varepsilon}_1 \\ \boldsymbol{\varepsilon}_2 \\ \boldsymbol{\gamma}_1 \\ \boldsymbol{\gamma}_2 \end{Bmatrix}; \quad \hat{\mathbf{D}} = \begin{bmatrix} \mathbf{A} & \mathbf{P} & \mathbf{C} & \mathbf{0} & \mathbf{0} \\ \mathbf{P} & \mathbf{H} & \mathbf{F} & \mathbf{0} & \mathbf{0} \\ \mathbf{C} & \mathbf{F} & \mathbf{G} & \mathbf{0} & \mathbf{0} \\ \mathbf{0} & \mathbf{0} & \mathbf{0} & \mathbf{A}_s & \mathbf{P}_s \\ \mathbf{0} & \mathbf{0} & \mathbf{0} & \mathbf{P}_s & \mathbf{C}_s \end{bmatrix}; \quad \bar{\mathbf{u}} = \begin{Bmatrix} \bar{\mathbf{u}}_1 \\ \bar{\mathbf{u}}_2 \\ \bar{\mathbf{u}}_3 \end{Bmatrix}; \quad \mathbf{m} = \begin{bmatrix} \mathbf{I}_0 & 0 & 0 \\ 0 & \mathbf{I}_0 & 0 \\ 0 & 0 & \mathbf{I}_0 \end{bmatrix} \tag{14}$$

where

$$\varepsilon_0 = \begin{Bmatrix} u_{,x} \\ v_{,y} \\ u_{,y} + v_{,x} \end{Bmatrix}; \varepsilon_1 = \begin{Bmatrix} \theta_{x,x} \\ \theta_{y,y} \\ \theta_{x,y} + \theta_{y,x} \end{Bmatrix}; \varepsilon_2 = \begin{Bmatrix} -w_{,xx} \\ -w_{,yy} \\ -2w_{,xy} \end{Bmatrix}; \gamma_1 = \begin{Bmatrix} \theta_x \\ \theta_y \end{Bmatrix}; \gamma_2 = \begin{Bmatrix} w_{,x} \\ w_{,y} \end{Bmatrix} \tag{15}$$

$$(\mathbf{A}, \mathbf{P}, \mathbf{C}) = \int_{z_b}^{z_t} (1, f(z), g(z))\,\mathbf{Q}_b dz \tag{16}$$

$$(\mathbf{H},\mathbf{F},\mathbf{G}) = \int_{z_b}^{z_t} \left((f(z))^2, f(z)\,g(z), (g(z))^2\right)\mathbf{Q}_b dz \tag{17}$$

$$(\mathbf{A}_s,\mathbf{P}_s,\mathbf{C}_s) = \int_{z_b}^{z_t} \left((f'(z))^2, (f'(z))(1-g'(z)), (1-g'(z))^2\right)\mathbf{Q}_s dz \tag{18}$$

$$\bar{\mathbf{u}}_1 = \begin{Bmatrix} u \\ v \\ w \end{Bmatrix}; \bar{\mathbf{u}}_2 = \begin{Bmatrix} \theta_x \\ \theta_y \\ 0 \end{Bmatrix}; \bar{\mathbf{u}}_3 = \begin{Bmatrix} -w_{,x} \\ -w_{,y} \\ 0 \end{Bmatrix}; \mathbf{I}_0 = \begin{bmatrix} I_1 & I_2 & I_3 \\ I_3 & I_4 & I_5 \\ I_3 & I_5 & I_6 \end{bmatrix} \tag{19}$$

$$(I_1,I_2,I_3,I_4,I_5,I_6) = \int_{z_b}^{z_t} \rho_e \left\{1, f(z), g(z), (f(z))^2, f(z)\,g(z), (g(z))^2\right\} dz \tag{20}$$

2.3. NURBS-based FEM formulations based on IGA

Developed by Hughes et al. [38] in 2005, IGA has penetrated various fields of engineering and research. It is widely demonstrated that IGA produces many preferable characteristics in terms of computational aspects, compared to the traditional FGM approach [39]. In the development of the IGA model, the basic component is the knot vector $\boldsymbol{\Xi}$, which is defined as a set of non-decreasing numbers

$$\boldsymbol{\Xi} = \left\{\xi_1,\ \xi_2,\ \xi_3, ...,\ \xi_i, ...,\ \xi_{n+p+1}\right\}, \quad \xi_i \le \xi_{i+1} \tag{21}$$

where ξ_i is the i^{th} knot in parametric space. The B-spline basis functions are developed in a recursive manner, starting with $p = 0$

$$N_{i,0}(\xi) = \begin{cases} 1 & \xi_i \le \xi < \xi_{i+1} \\ 0 & \text{otherwise} \end{cases} \tag{22}$$

and for other $p \ge 1$ as follows

$$N_{i,p} = \frac{\xi - \xi_i}{\xi_{i+p} - \xi_i} N_{i,p-1}(\xi) + \frac{\xi_{i+p+1} - \xi}{\xi_{i+p+1} - \xi_{i+1}} N_{i,p-1}(\xi) \tag{23}$$

For 2-Dimensional (2D) problems, 2D NURBS basis functions are constructed based on tensor products of two or univariate B-spline basis functions ($N_{i,p}(\xi)$ and $M_{i,q}(\eta)$) as follows:

$$R_{i,j}^{p,q}(\xi,\eta) = \frac{N_{i,p}(\xi)\,M_{i,q}(\eta)\,w_{ij}}{W(\xi,\eta)} = \frac{N_{i,p}(\xi)\,M_{i,q}(\eta)\,w_{i,j}}{\sum_{\hat{i}=1}^{n}\sum_{\hat{j}=1}^{m} N_{\hat{i},p}(\xi) M_{\hat{j},q}(\eta)\,w_{\hat{i},\hat{j}}} \tag{24}$$

By adopting NURBS basis functions as interpolation functions, the displacement variables can be interpolated as

$$\mathbf{u} = \sum_{i=1}^{ncp} R_i(\xi,\mu)\,\mathbf{d}_i \tag{25}$$

where $\mathbf{u} = \begin{Bmatrix} u & v & \theta_x & \theta_y & w \end{Bmatrix}^T$; $\mathbf{d}_i = \begin{Bmatrix} u_i & v_i & \theta_{xi} & \theta_{yi} & w_i \end{Bmatrix}^T$. Substituting Eq. (25) into Eq. (15), the strain vectors can be represented as follows

$$\hat{\boldsymbol{\varepsilon}} = \begin{Bmatrix} \boldsymbol{\varepsilon}_0 \\ \boldsymbol{\varepsilon}_1 \\ \boldsymbol{\varepsilon}_2 \\ \boldsymbol{\gamma}_1 \\ \boldsymbol{\gamma}_2 \end{Bmatrix} = \sum_{i}^{ncp} \begin{Bmatrix} \mathbf{B}_{\varepsilon 0} \\ \mathbf{B}_{\varepsilon 1} \\ \mathbf{B}_{\varepsilon 2} \\ \mathbf{B}_{\gamma 1} \\ \mathbf{B}_{\gamma 2} \end{Bmatrix} \mathbf{d} \tag{26}$$

in which

$$\mathbf{B}_{\varepsilon 0} = \begin{bmatrix} R_{,x} & 0 & 0 & 0 & 0 \\ 0 & R_{,y} & 0 & 0 & 0 \\ R_{,y} & R_{,x} & 0 & 0 & 0 \end{bmatrix}; \quad \mathbf{B}_{\varepsilon 1} = \begin{bmatrix} 0 & 0 & R_{,x} & 0 & 0 \\ 0 & 0 & 0 & R_{,y} & 0 \\ 0 & 0 & R_{,y} & R_{,x} & 0 \end{bmatrix} \tag{27}$$

$$\mathbf{B}_{\varepsilon 2} = \begin{bmatrix} 0 & 0 & 0 & 0 & -R_{,xx} \\ 0 & 0 & 0 & 0 & -R_{,yy} \\ 0 & 0 & 0 & 0 & -2R_{,xy} \end{bmatrix} \tag{28}$$

$$\mathbf{B}_{\gamma 1} = \begin{bmatrix} 0 & 0 & R & 0 & 0 \\ 0 & 0 & 0 & R & 0 \end{bmatrix}; \quad \mathbf{B}_{\gamma 2} = \begin{bmatrix} 0 & 0 & 0 & 0 & R_{,x} \\ 0 & 0 & 0 & 0 & R_{,y} \end{bmatrix} \tag{29}$$

It is seen that the construction of the $\mathbf{B}_{\varepsilon 2}$ matrix requires interpolation functions with C^2-continuity. This requirement is treated efficiently based on the IGA concept [38]. Then, the system equations for linear bending are developed from Eq. (12) and can be written as follows

$$\mathbf{K}\mathbf{d} = \mathbf{f}_q \tag{30}$$

For the free vibration analysis, the harmonic vibrations are assumed and hence the system equation can be developed as follows

$$\left(\mathbf{K} - \omega^2 \mathbf{M}\right)\mathbf{d} = \mathbf{0} \tag{31}$$

in which the stiffness matrix $\mathbf{K}$, distributed force vector $\mathbf{f}$, and mass matrix $\mathbf{M}$ are written as

$$\mathbf{K} = \int_{\Omega} \mathbf{B}_T^T \hat{\mathbf{D}} \mathbf{B} d\Omega \tag{32}$$

$$\mathbf{f}_q = \int_{\Omega} q(x,y) \begin{Bmatrix} 0 & 0 & 0 & 0 & R \end{Bmatrix}^T d\Omega \tag{33}$$

$$\mathbf{M} = \int_{\Omega} \hat{\mathbf{R}}_{mT} \mathbf{m} \hat{\mathbf{R}}_m d\Omega \tag{34}$$

where

$$\mathbf{B} = \begin{Bmatrix} \mathbf{B}_{\varepsilon 0} \\ \mathbf{B}_{\varepsilon 1} \\ \mathbf{B}_{\varepsilon 2} \\ \mathbf{B}_{\gamma 1} \\ \mathbf{B}_{\gamma 2} \end{Bmatrix}; \quad \mathbf{B}_T = \begin{Bmatrix} \mathbf{B}_{\varepsilon 1}^T \\ \mathbf{B}_{\varepsilon 1}^T \\ \mathbf{B}_{\varepsilon 2}^T \\ \mathbf{B}_{\gamma 1}^T \\ \mathbf{B}_{\gamma 2}^T \end{Bmatrix} \tag{35}$$

$$\mathbf{R}_{m1} = \begin{bmatrix} R & 0 & 0 & 0 & 0 \\ 0 & R & 0 & 0 & 0 \\ 0 & 0 & 0 & 0 & R \end{bmatrix}; \quad \mathbf{R}_{m2} = \begin{bmatrix} 0 & 0 & R & 0 & 0 \\ 0 & 0 & 0 & R & 0 \\ 0 & 0 & 0 & 0 & 0 \end{bmatrix} \tag{36}$$

$$\mathbf{R}_{m3} = \begin{bmatrix} 0 & 0 & 0 & 0 & -R_{,x} \\ 0 & 0 & 0 & 0 & -R_{,y} \\ 0 & 0 & 0 & 0 & 0 \end{bmatrix} \tag{37}$$

3. Numerical examples

3.1. Verifications

In this section, the accuracy of the proposed approach is validated by revisiting some numerical examples regarding variable thickness plates and MFGM plates that were published in the literature.

In the first validation example, the free vibration problem of an isotropic square plate is considered. The reference solutions were developed by Shufrin and Eisenberger [40] based on the extended Kantorovich method, Mizusawa [41] by spline strip method, and Bacciocchi et al. [42] by differential quadrature method. It is assumed that the thickness of the square plate is simply supported by the SSSS boundary condition and it has a linear variation in x-direction, where the thickness profile is given by the following relation

$$h(x) = h_0\left(1 - \frac{x}{2a}\right) \tag{38}$$

or

$$z_t(x, y) = -z_b(x, y) = \frac{h_0}{2}\left(1 - \frac{x}{2a}\right) \tag{39}$$

Details of SSSS boundary conditions are

$$\begin{aligned} u = \theta_x = w = 0 \text{ at } y = 0 \text{ and } y = b \\ v = \theta_y = w = 0 \text{ at } x = 0 \text{ and } x = a \end{aligned} \tag{40}$$

The frequencies are expressed in terms of the dimensionless factor

$$\bar{\omega} = \frac{\omega a^2}{\pi^2}\sqrt{\frac{12\rho(1-\nu^2)}{Eh_0^2}} \tag{41}$$

where ρ is the material density, E is Young's modulus and ν is the Poisson's ratio taken as 0.3. In Table 1, the results of natural frequencies of the plate obtained from the present approach are compared with those referenced ones. It is seen that the proposed model numerical model based on

Table 1. Comparison of natural frequencies for SSSS square plate with linearly variable thickness in x-direction

h_0/a	Studies	Mode							
		1,1	1,2	2,1	2,2	1,3	3,1	3,2	2,3
0.1	Shufrin and Eisenberger [40]	1.4504	3.4743	3.5058	5.4838	6.5345	6.7038	8.5303	8.5921
	Mizusawa [41]	1.4504	3.4743	3.5058	5.4840	6.5347	6.7039	8.5302	-
	Bacciocchi et al. [42]	1.4507	3.4758	3.5074	5.4876	6.5394	6.7093	8.5390	8.6009
	Present	1.4507	3.4759	3.5075	5.4880	6.5401	6.7101	8.5406	8.6026
0.2	Shufrin and Eisenberger [40]	1.3738	3.1096	3.1276	4.6613	5.4883	5.5657	6.8435	6.8725
	Mizusawa [41]	1.3738	3.1096	3.1276	4.6613	5.4881	5.5656	6.8437	6.8726
	Bacciocchi et al. [42]	1.3747	3.1139	3.1320	4.6703	5.4996	5.5778	6.8607	6.8900
	Present	1.3749	3.1150	3.1331	4.6741	5.5049	5.5841	6.8722	6.9019
0.4	Shufrin and Eisenberger [40]	1.1664	2.3603	2.3637	3.2845	3.7942	3.8050	4.5043	4.5105
	Mizusawa [41]	1.1665	2.3603	2.3637	3.2845	3.7942	3.8050	4.5043	4.5105
	Bacciocchi et al. [42]	1.1687	2.3675	2.3710	3.2969	3.8093	3.8204	4.5241	4.5304
	Present	1.1696	2.3744	2.3782	3.3157	3.8352	3.8488	4.5708	4.5772

IGA yields good-agreement solutions with other approaches. It is noted that the current solutions are obtained from a mesh of 12×12 with cubic basis functions ($p = q = 3$). This mesh size is obtained from a convergence study, which is omitted for a brief purpose, and the mesh will be used henceforward.

In the second validation example, the free vibration of a square and uniform-thickness MFGM plate with a spatial gradation of material constituent is revisited. The problem was firstly addressed by Thai and Thai [43] by using the 3D IGA approach to solve the general elasticity problems. It is assumed that the plate has side length a, thickness $h = a/10$, and is clamped at four edges with CCCC boundary condition

$$u = v = \theta_x = \theta_y = w = \frac{\partial w}{\partial n} = 0 \text{ at all edges} \tag{42}$$

The plate is made from Al_2O_3 (ceramic) and Al (metal), where $E_c = 380$ GPa, $\rho_c = 3800$ kg/m^3, $E_m = 70$ GPa, $\rho_m = 2707$ kg/m^3, and $\nu_c = \nu_m = 0.3$. The volume fraction of ceramic constituent is expressed as follows

$$V_c = \left\{\frac{4x}{a}\left(1 - \frac{x}{a}\right)\right\}^{n_x}\left\{\frac{4y}{b}\left(1 - \frac{y}{b}\right)\right\}^{n_y}\left(\frac{z}{h} + \frac{1}{2}\right)^{n_z} \tag{43}$$

where n_x, n_y, and n_z are the gradient indices in three spatial directions. The non-dimensional natural frequency is given by

$$\bar{\omega} = \frac{\omega a^2}{h^2}\sqrt{\frac{\rho_c}{E_c}} \tag{44}$$

As can be seen in Table 2, the results obtained from the current approach are in good agreement with those obtained from the 3D IGA approach.

Table 2. Comparison of natural frequencies of uniform-thickness square MFGM plate with clamped boundary conditions

	$n = n_x = n_y = n_z$							
	0		1		2		100	
	3D IGA [43]	Present	3D IGA [43]	Present	3D IGA [43]	Present	3D IGA [43]	Present
$\bar{\omega}_1$	10.6742	10.6010	6.6877	6.6345	6.1573	6.1113	5.4296	5.3976
$\bar{\omega}_2$	21.3315	21.1995	13.7138	13.6358	12.4436	12.3641	10.8477	10.7815
$\bar{\omega}_3$	30.8881	30.7316	19.7475	19.6792	17.8457	17.7577	15.7096	15.6381
$\bar{\omega}_4$	37.2134	36.9999	24.3297	24.2598	21.8867	21.7719	18.9272	18.8304

In the third validation example, the bending problem of the isotropic plate ($E = 1$ GPa, $\nu = 0.3$) with variable thickness is revisited. It is supposed that the rectangular plate has non-uniform thickness $h(x)$ along x-direction. The plate is subjected to uniformly distributed load and the boundary condition is CSCS (clamped at $x = 0$ and $x = a$, simply supported at $y = 0$ and $y = a$, which is inversed x, y order in the referenced study [13]). It is assumed that $h_0 = 0.001a = h_{\min}, h_{\max} = 1.2h_0$. The thickness of the plates is expressed by

$$h(x) = h_0\left[1 + \lambda\left(\frac{2x}{a} - 1\right)^2\right] \tag{45}$$

where λ is a factor representing the variation of the plates' thickness. For $\lambda = 2$, the coordinate of the

top and bottom surface of the plates is given by

$$z_t(x,y) = \frac{h_{\min}}{2}; \quad z_b(x,y) = -h_{\max} + \frac{h_{\min}}{2} - 4\left(h_{\max} - h_{\min}\right)\left\{\left(\frac{x}{a}\right)^2 - \frac{x}{a}\right\} \tag{46}$$

Details of the CSCS boundary condition are given by

$$\begin{array}{ll} u = \theta_x = w = 0 & \text{at } y = 0 \text{ and } y = b \\ u = v = \theta_x = \theta_y = w = 0 & \text{at } x = 0 \text{ and } x = a \end{array} \tag{47}$$

Table 3. Comparison of deflection results $\bar{w}$ of the rectangular isotropic plate with variable thickness

a/b	$\lambda = 0$		$\lambda = 2$	
	Zenkour [13]	Present	Zenkour [13]	Present
1.0	1.9171	1.9155	1.5585	1.5364
1.2	3.1944	3.1928	2.6498	2.6230
1.4	4.6128	4.6145	3.9040	3.8789
1.6	6.0221	6.0296	5.1934	5.1754
1.8	7.3171	7.3319	6.4173	6.4090
2.0	8.4450	8.4665	7.5160	7.5172

As shown in Table 3, the deflection results obtained from the current approach and referenced ones agree well with each other. The non-dimensional quantities are calculated as follows

$$\bar{w} = \frac{10^3 D_0}{q_0 b^4} w\left(\frac{a}{2}, \frac{b}{2}\right); \quad D_0 = \frac{E h_0^3}{12\left(1 - \nu^2\right)} \tag{48}$$

3.2. Parametric investigations

In this section, parametric investigations are conducted to study the influence of geometrical and material parameters on the linear bending and free vibration responses of MFGM plates with variable thickness as shown in Fig. 1. To demonstrate the efficiency of the IGA approach in the modelling aspect, circular plates are also investigated along with rectangular plates. Both rectangular and circular plates are assumed to be made from Al_2O_3 (E_c = 380 GPa, ρ_c = 3800 kg/m^3, ν_c = 0.3) and Al (E_m = 70 GPa, ρ_m = 2707 kg/m^3, ν_m = 0.3).

For rectangular plates with side lengths a (along x-direction) and b (along y-direction), the spatial distribution of ceramic volume fraction is given by Eq. (49)

$$V_c = \left\{\frac{4x}{a}\left(1 - \frac{x}{a}\right)\right\}^{n_x}\left\{\frac{4y}{b}\left(1 - \frac{y}{b}\right)\right\}^{n_y}\left(\frac{z - z_b(x,y)}{h(x,y)}\right)^{n_z} \tag{49}$$

where n_x, n_y and n_z are volume fraction indices. The coordinate of the top and bottom surfaces of the plates follow the expression in Eq. (46), and the nondimensional results are expressed in Eq. (50).

$$\bar{w} = \frac{10^3 D_0}{q_0 a^4} w\left(\frac{a}{2}, \frac{b}{2}\right); \quad D_0 = \frac{E_c h_{\min}^3}{12\left(1 - \nu_c^2\right)}; \quad \bar{\omega} = \frac{\omega a^2}{h_{\min}}\sqrt{\frac{\rho_c}{E_c}} \tag{50}$$

For circular plates with radius R, the spatial variation of ceramic volume fraction is expressed by

$$V_c = \left(1 - \frac{r}{R}\right)^{n_r} \left(\frac{z - z_b(x,y)}{h(x,y)}\right)^{n_z} \tag{51}$$

where n_r and n_z are the volume fraction indices in the radius and thickness directions. The coordinates of the top and bottom surfaces are given as follows

$$z_t(x,y) = \frac{h_{\min}}{2}; \quad z_b(x,y) = -\frac{h_{\min}}{2} - \left\{1 - \left(\frac{r}{R}\right)^2\right\}(h_{\max} - h_{\min}) \tag{52}$$

in which $r = \sqrt{x^2 + y^2}$. The non-dimensional quantities for circular plates are given by

$$\bar{w} = \frac{64 D_0}{q_0 R^4} w(0,0); \quad \bar{\omega} = \omega R^2 \sqrt{\frac{\rho_c h_{\min}}{D_0}}; \quad D_0 = \frac{E_c h_{\min}^3}{12\left(1 - \nu_c^2\right)} \tag{53}$$

Two boundary conditions for circular plates are simply supported (Sr) and clamped (Cr) boundaries. Expressions for those are given in Eqs. (54) and (55), respectively.

$$u = v = w = 0 \qquad \text{at the boundary} \tag{54}$$

$$u = v = \theta_x = \theta_y = w = \frac{\partial w}{\partial n} = 0 \qquad \text{at the boundary} \tag{55}$$

In Tables 4 and 5, the deflection results of rectangular MFGM plates with different gradient indices, plates' geometry aspects a/b, and thickness ratios $h_{\min}/h_{\max}$ are presented. The deflection results for circular MFGM plates are also presented in Table 6. In general, it can be seen that the increase of gradient indices (n_x, n_y, or n_z) leads to an increase in bending results. This is due to the rise of the metal constituent within the plate's domain, and hence reduces the stiffness of the plates. Additionally, it is seen that the bending results decrease with the increases in thickness ratios and plates' aspect ratios.

Table 4. Defelction results of SSSS rectangular MFGM plates ($h_{\min} = a/10, a = 1$ m)

$h_{\max}/h_{\min}$	n_z	n_y	$a/b = 1$					$b/a = 2$				
			n_x					n_x				
			0	0.5	1	2	10	0	0.5	1	2	10
1.5	0	0	2.9330	3.5517	4.0599	4.8473	7.7912	0.5571	0.6268	0.6859	0.7805	1.1661
		0.5	3.5778	4.1574	4.6204	5.3384	8.0856	0.6677	0.7326	0.7868	0.8746	1.2460
		1	4.1439	4.6729	5.0965	5.7601	8.3567	0.7738	0.8340	0.8845	0.9673	1.3254
		2	5.0433	5.4921	5.8582	6.4441	8.8184	0.9495	1.0030	1.0484	1.1239	1.4588
		10	8.2014	8.4376	8.6511	9.0209	10.6758	1.6113	1.6429	1.6710	1.7202	1.9560
	0.5	0	4.5113	5.2624	5.8267	6.6409	9.3284	0.8476	0.9336	1.0021	1.1069	1.5022
		0.5	5.2898	5.9510	6.4417	7.1563	9.6060	0.9815	1.0576	1.1182	1.2126	1.5830
		1	5.9078	6.4896	6.9252	7.5688	9.8471	1.0968	1.1651	1.2200	1.3069	1.6563
		2	6.8184	7.2903	7.6525	8.2018	10.2416	1.2735	1.3314	1.3789	1.4554	1.7724
		10	9.6891	9.9126	10.1042	10.4223	11.7682	1.8646	1.8955	1.9226	1.9688	2.1772

h_{max}/h_{min}	n_z	n_y	$a/b = 1$					$b/a = 2$				
			n_x					n_x				
			0	0.5	1	2	10	0	0.5	1	2	10
		0	5.8650	6.6175	7.1544	7.9008	10.2517	1.0977	1.1857	1.2535	1.3553	1.7253
		0.5	6.6439	7.2777	7.7308	8.3727	10.4986	1.2351	1.3106	1.3693	1.4594	1.8004
	1	1	7.2260	7.7710	8.1667	8.7385	10.7080	1.3462	1.4125	1.4650	1.5467	1.8647
		2	8.0508	8.4831	8.8069	9.2899	11.0475	1.5088	1.5638	1.6082	1.6789	1.9638
		10	10.5610	10.7607	10.9291	11.2055	12.3594	2.0257	2.0541	2.0788	2.1205	2.3038
		0	7.5534	8.1874	8.6319	9.2413	11.1561	1.4175	1.4947	1.5542	1.6431	1.9603
		0.5	8.2096	8.7285	9.0978	9.6193	11.3578	1.5410	1.6064	1.6573	1.7349	2.0232
	2	1	8.6854	9.1262	9.4469	9.9113	11.5285	1.6361	1.6928	1.7377	1.8073	2.0742
		2	9.3511	9.6991	9.9617	10.3557	11.8079	1.7707	1.8172	1.8548	1.9143	2.1520
		10	11.4038	11.5697	11.7099	11.9406	12.9065	2.1928	2.2168	2.2375	2.2723	2.4244
		0	10.1101	10.6296	10.9868	11.4584	12.8239	1.9610	2.0250	2.0732	2.1424	2.3692
		0.5	10.6344	11.0524	11.3423	11.7372	12.9622	2.0488	2.1017	2.1415	2.1999	2.4024
	10	1	11.0070	11.3571	11.6045	11.9508	13.0798	2.1127	2.1577	2.1921	2.2437	2.4300
		2	11.5175	11.7880	11.9856	12.2729	13.2718	2.2026	2.2386	2.2667	2.3100	2.4747
		10	12.9990	13.1188	13.2165	13.3735	14.0050	2.4834	2.5007	2.5152	2.5392	2.6414
		0	2.0208	2.5228	2.9324	3.5430	5.6256	0.4384	0.4983	0.5491	0.6296	0.9492
		0.5	2.5382	3.0268	3.4031	3.9521	5.8426	0.5338	0.5922	0.6397	0.7144	1.0163
	0	1	3.0076	3.4562	3.7957	4.2905	6.0339	0.6250	0.6802	0.7246	0.7946	1.0810
		2	3.7412	4.1142	4.3957	4.8116	6.3474	0.7735	0.8227	0.8623	0.9250	1.1870
		10	6.0741	6.2360	6.3694	6.5872	7.5530	1.2976	1.3260	1.3497	1.3891	1.5655
		0	3.1389	3.7337	4.1693	4.7701	6.5945	0.6702	0.7425	0.7996	0.8857	1.2036
		0.5	3.7512	4.2806	4.6554	5.1706	6.7901	0.7848	0.8501	0.9006	0.9776	1.2699
	0.5	1	4.2396	4.7012	5.0270	5.4790	6.9541	0.8822	0.9409	0.9864	1.0564	1.3284
		2	4.9395	5.3031	5.5629	5.9322	7.2155	1.0279	1.0772	1.1160	1.1765	1.4190
		10	6.9647	7.1106	7.2271	7.4131	8.2045	1.4881	1.5137	1.5352	1.5707	1.7254
		0	4.0989	4.6788	5.0776	5.6081	7.1657	0.8693	0.9416	0.9965	1.0780	1.3703
		0.5	4.6967	5.1825	5.5129	5.9579	7.3353	0.9853	1.0476	1.0950	1.1662	1.4311
2	1	1	5.1391	5.5504	5.8327	6.2199	7.4753	1.0775	1.1320	1.1739	1.2378	1.4819
		2	5.7480	6.0639	6.2863	6.6016	7.6986	1.2094	1.2540	1.2889	1.3433	1.5588
		10	7.4753	7.6016	7.7028	7.8652	8.5536	1.6090	1.6313	1.6501	1.6814	1.8169
		0	5.3037	5.7684	6.0818	6.4961	7.7333	1.1243	1.1854	1.2319	1.3010	1.5472
		0.5	5.7853	6.1595	6.4148	6.7620	7.8685	1.2264	1.2778	1.3172	1.3769	1.5977
	2	1	6.1289	6.4412	6.6588	6.9626	7.9813	1.3038	1.3481	1.3826	1.4356	1.6379
		2	6.5980	6.8374	7.0103	7.2615	8.1647	1.4115	1.4472	1.4757	1.5205	1.6984
		10	7.9794	8.0814	8.1654	8.3023	8.8875	1.7365	1.7544	1.7696	1.7951	1.9068
		0	7.1481	7.5063	7.7467	8.0520	8.8867	1.5660	1.6151	1.6519	1.7044	1.8730
		0.5	7.5074	7.7918	7.9834	8.2345	8.9761	1.6384	1.6786	1.7087	1.7523	1.8999
	10	1	7.7599	7.9947	8.1558	8.3729	9.0521	1.6902	1.7242	1.7499	1.7878	1.9218
		2	8.0999	8.2775	8.4033	8.5800	9.1762	1.7614	1.7881	1.8087	1.8399	1.9565
		10	9.0615	9.1343	9.1924	9.2841	9.6549	1.9741	1.9864	1.9966	2.0133	2.0834

Table 5. Deflection results of CCCC rectangular MFGM plates ($h_{\min} = a/10, a = 1$ m)

$h_{\max}/h_{\min}$	n_z	n_y	$a/b = 1$					$b/a = 2$				
			n_x					n_x				
			0	0.5	1	2	10	0	0.5	1	2	10
1.5	0	0	1.0183	1.2743	1.4749	1.7215	2.4557	0.2125	0.2255	0.2361	0.2533	0.3449
		0.5	1.2022	1.5308	1.7834	2.0773	2.8447	0.2947	0.3152	0.3306	0.3534	0.4584
		1	1.3363	1.7108	1.9924	2.3069	3.0607	0.3657	0.3920	0.4104	0.4356	0.5414
		2	1.5108	1.9288	2.2318	2.5540	3.2617	0.4589	0.4909	0.5115	0.5368	0.6334
		10	2.1448	2.6245	2.9312	3.2211	3.7549	0.6780	0.7126	0.7311	0.7498	0.8106
	0.5	0	1.5520	1.8501	2.0589	2.3116	3.0304	0.3147	0.3303	0.3428	0.3630	0.4648
		0.5	1.7797	2.1356	2.3768	2.6540	3.3593	0.4125	0.4337	0.4493	0.4728	0.5781
		1	1.9343	2.3202	2.5753	2.8584	3.5325	0.4876	0.5121	0.5290	0.5530	0.6531
		2	2.1294	2.5378	2.7986	3.0766	3.6974	0.5797	0.6066	0.6237	0.6462	0.7334
		10	2.7884	3.1950	3.4288	3.6562	4.1066	0.7777	0.8017	0.8147	0.8294	0.8814
	1	0	2.0099	2.3038	2.5009	2.7385	3.3951	0.4040	0.4201	0.4329	0.4537	0.5554
		0.5	2.2458	2.5778	2.7932	3.0415	3.6682	0.5046	0.5244	0.5390	0.5613	0.6604
		1	2.4012	2.7502	2.9716	3.2192	3.8121	0.5776	0.5990	0.6140	0.6358	0.7271
		2	2.5929	2.9509	3.1712	3.4094	3.9512	0.6633	0.6853	0.6997	0.7194	0.7969
		10	3.2114	3.5428	3.7300	3.9169	4.3035	0.8370	0.8549	0.8651	0.8774	0.9223
	2	0	2.5982	2.8512	3.0208	3.2238	3.7718	0.5281	0.5430	0.5551	0.5749	0.6685
		0.5	2.8141	3.0850	3.2619	3.4665	3.9821	0.6229	0.6395	0.6522	0.6720	0.7581
		1	2.9551	3.2326	3.4102	3.6107	4.0953	0.6881	0.7051	0.7175	0.7360	0.8128
		2	3.1239	3.4019	3.5753	3.7651	4.2055	0.7596	0.7761	0.7875	0.8035	0.8673
		10	3.6513	3.8986	4.0414	4.1861	4.4959	0.8967	0.9095	0.9172	0.9268	0.9633
	10	0	3.6415	3.8437	3.9693	4.1080	4.4502	0.8029	0.8155	0.8251	0.8397	0.9003
		0.5	3.8197	4.0249	4.1486	4.2803	4.5845	0.8711	0.8833	0.8922	0.9049	0.9543
		1	3.9265	4.1297	4.2494	4.3737	4.6509	0.9087	0.9201	0.9281	0.9391	0.9809
		2	4.0471	4.2431	4.3553	4.4686	4.7139	0.9417	0.9520	0.9588	0.9679	1.0023
		10	4.4099	4.5673	4.6507	4.7296	4.8923	1.0017	1.0088	1.0132	1.0186	1.0399
2	0	0	0.7113	0.8944	1.0493	1.2481	1.8103	0.1865	0.1991	0.2096	0.2263	0.3090
		0.5	0.8163	1.0423	1.2304	1.4619	2.0425	0.2528	0.2725	0.2878	0.3098	0.4046
		1	0.8944	1.1473	1.3539	1.6002	2.1706	0.3095	0.3348	0.3533	0.3781	0.4740
		2	1.0012	1.2810	1.5021	1.7554	2.2949	0.3845	0.4158	0.4370	0.4630	0.5519
		10	1.4145	1.7374	1.9645	2.2003	2.6237	0.5680	0.6036	0.6244	0.6461	0.7054
	0.5	0	1.0968	1.3059	1.4587	1.6496	2.1784	0.2776	0.2924	0.3042	0.3231	0.4135
		0.5	1.2295	1.4710	1.6426	1.8481	2.3661	0.3568	0.3768	0.3916	0.4136	0.5075
		1	1.3215	1.5797	1.7591	1.9681	2.4657	0.4175	0.4406	0.4568	0.4795	0.5696
		2	1.4436	1.7146	1.8972	2.1031	2.5657	0.4929	0.5186	0.5353	0.5573	0.6371
		10	1.8841	2.1542	2.3198	2.4930	2.8404	0.6628	0.6866	0.7003	0.7161	0.7656
	1	0	1.4266	1.6264	1.7641	1.9352	2.4074	0.3566	0.3714	0.3832	0.4022	0.4917
		0.5	1.5644	1.7840	1.9311	2.1073	2.5596	0.4382	0.4562	0.4697	0.4901	0.5779
		1	1.6574	1.8854	2.0350	2.2103	2.6413	0.4973	0.5168	0.5308	0.5510	0.6328
		2	1.7779	2.0099	2.1583	2.3273	2.7253	0.5680	0.5883	0.6020	0.6206	0.6913
		10	2.1946	2.4086	2.5358	2.6716	2.9648	0.7187	0.7358	0.7460	0.7585	0.8008
	2	0	1.8484	2.0111	2.1226	2.2617	2.6471	0.4657	0.4789	0.4897	0.5072	0.5890
		0.5	1.9736	2.1441	2.2584	2.3972	2.7624	0.5422	0.5568	0.5681	0.5858	0.6619
		1	2.0574	2.2303	2.3442	2.4801	2.8262	0.5951	0.6100	0.6211	0.6379	0.7067
		2	2.1631	2.3352	2.4462	2.5754	2.8932	0.6546	0.6692	0.6796	0.6944	0.7523
		10	2.5186	2.6712	2.7636	2.8646	3.0946	0.7750	0.7866	0.7939	0.8034	0.8371

h_{max}/h_{min}	n_z	n_y	$a/b = 1$					$b/a = 2$				
			n_x					n_x				
			0	0.5	1	2	10	0	0.5	1	2	10
		0	2.5942	2.7204	2.8025	2.8973	3.1227	0.7081	0.7191	0.7276	0.7407	0.7924
		0.5	2.6954	2.8221	2.9024	2.9924	3.1953	0.7623	0.7730	0.7809	0.7924	0.8353
	10	1	2.7584	2.8834	2.9610	3.0465	3.2330	0.7928	0.8028	0.8100	0.8201	0.8568
		2	2.8341	2.9545	3.0275	3.1060	3.2723	0.8209	0.8301	0.8363	0.8448	0.8749
		10	3.0787	3.1760	3.2310	3.2868	3.3985	0.8759	0.8824	0.8864	0.8915	0.9095

Table 6. Deflection results of circular MFGM plates ($h_{min} = R/10, R = 1$ m)

BCs	h_{max}/h_{min}	n_z	n_r				
			0	0.5	1	2	10
Sr	1.5	0	1.4706	2.0366	2.6489	3.7821	6.9855
		0.5	2.5066	3.2260	3.8997	4.9689	7.3568
		1	3.3212	4.0849	4.7323	5.6697	7.5292
		2	4.2228	4.9705	5.5401	6.2954	7.6606
		10	5.5938	6.1623	6.5460	7.0154	7.8041
	2	0	0.6295	0.9059	1.2028	1.7189	3.0294
		0.5	1.1353	1.4843	1.7991	2.2619	3.1902
		1	1.5794	1.9309	2.2136	2.5916	3.2656
		2	2.1091	2.4107	2.6253	2.8886	3.3217
		10	2.7203	2.8998	3.0141	3.1484	3.3675
	4	0	0.0804	0.1320	0.1839	0.2570	0.3987
		0.5	0.1489	0.2133	0.2640	0.3232	0.4164
		1	0.2149	0.2775	0.3196	0.3636	0.4249
		2	0.3043	0.3498	0.3757	0.4001	0.4310
		10	0.3981	0.4112	0.4177	0.4243	0.4343
Cr	1.5	0	0.5303	0.9129	1.2097	1.5736	2.5068
		0.5	0.8171	1.2789	1.5877	1.9228	2.6326
		1	1.0632	1.5364	1.8277	2.1223	2.6910
		2	1.3702	1.8065	2.0603	2.3006	2.7364
		10	1.8331	2.2039	2.3826	2.5363	2.7978
	2	0	0.3003	0.5090	0.6759	0.8915	1.4327
		0.5	0.4685	0.7311	0.9106	1.1089	1.5073
		1	0.6133	0.8912	1.0637	1.2357	1.5419
		2	0.7962	1.0626	1.2135	1.3486	1.5678
		10	1.0744	1.2954	1.3935	1.4720	1.5957
	4	0	0.0607	0.1026	0.1412	0.1927	0.2979
		0.5	0.0993	0.1548	0.1960	0.2403	0.3119
		1	0.1329	0.1940	0.2328	0.2687	0.3185
		2	0.1767	0.2374	0.2694	0.2939	0.3233
		10	0.2443	0.2876	0.3031	0.3133	0.3265

As depicted in Fig. 2(a), the influence of in-plane gradient indices (n_x and n_y) and thickness index (n_z) are different. The influence of thickness gradient index (n_z) is more pronounced when $n_z < 5$, where the deflection results change considerably. For the in-plane gradient indices, their effects on deflection results are less significant when the thickness gradient index is relatively large (e.g. $n_z = 5$).

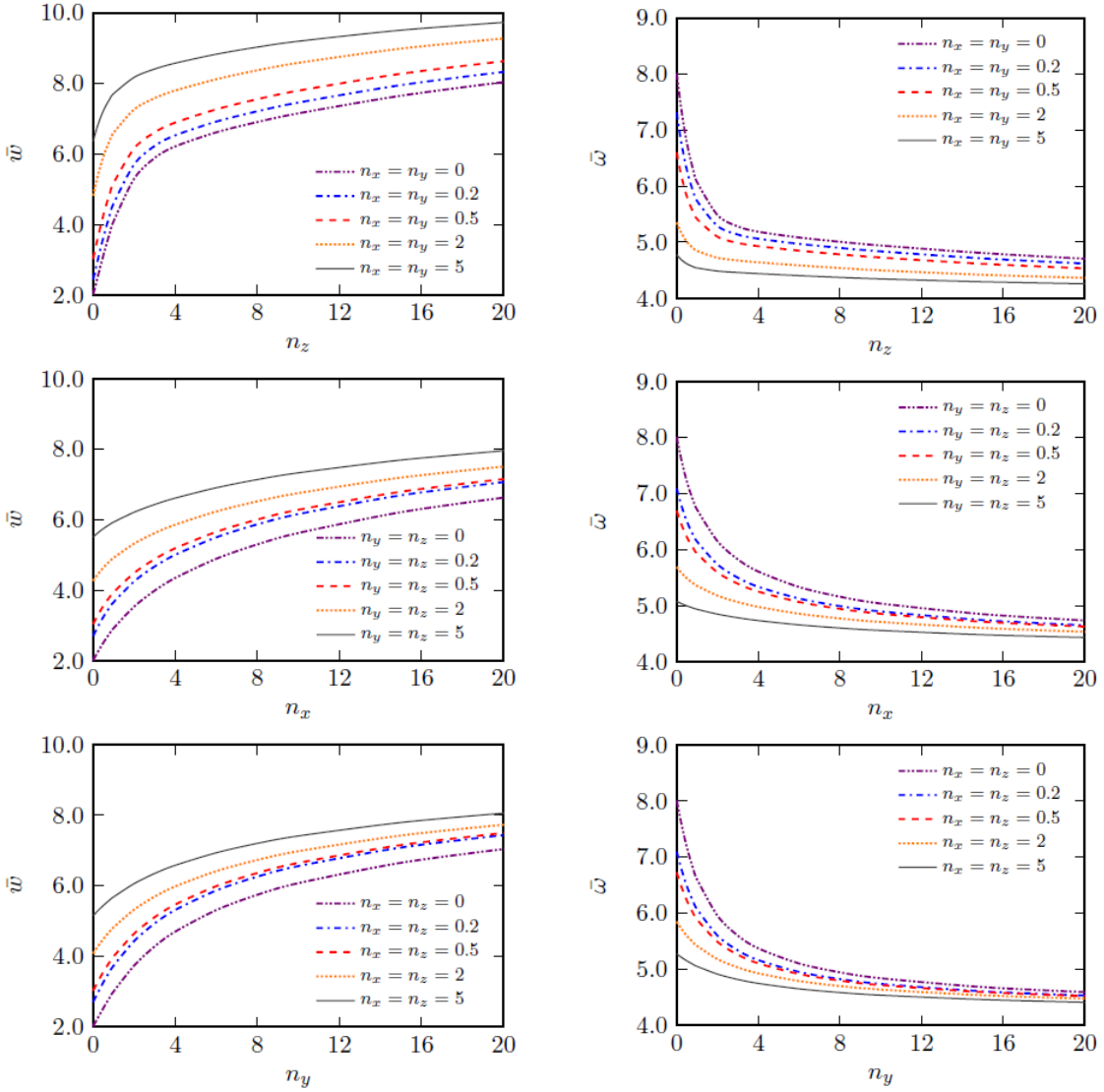

(a) Deflection results

(b) Nondimensional fundamental natural frequency results

Figure 2. Influence of gradient indices on the deflection and fundamental natural frequency results of square SSSS MFGM plates (a = 1 m, $h_{\min}$ = 0.1 m, $h_{\max} = 2h_{\min}$)

The results of non-dimensional fundamental natural frequencies of rectangular MFGM plates are tabulated in Tables 7 and 8, while the results for circular plates are presented in Table 9. Overall, the free vibration results decrease with the increase of gradient indices. As explained earlier, the elevation of gradient indices makes the volume fraction of ceramic reduce, hence, decreasing the stiffness of the plates and consequently the fundamental frequency of the plate decrease. In Fig. 2(b), the influences of each gradient index are illustrated. Similar to the observation on bending response, it is seen that the thickness gradient index has a noticeable effect on the free vibration response only when it is smaller than 5. Additionally, the changes in free vibration results are less steep when only in-plane gradient indices are elevated.

Table 7. Nondimensional fundamental natural frequency results of SSSS rectangular MFGM plates ($h_{\min} = a/10, a = 1$ m)

$h_{\max}/h_{\min}$	n_z	n_y	$a/b = 1$					$b/a = 2$				
			n_x					n_x				
			0	0.5	1	2	10	0	0.5	1	2	10
1.5	0	0	6.8041	6.2155	5.8389	5.3835	4.3912	4.1362	3.8633	3.6808	3.4352	2.7571
		0.5	6.1877	5.7733	5.5015	5.1561	4.3250	3.8519	3.6590	3.5216	3.3237	2.7251
		1	5.7718	5.4680	5.2602	4.9839	4.2656	3.6514	3.5103	3.4018	3.2357	2.6960
		2	5.2694	5.0795	4.9404	4.7427	4.1704	3.3985	3.3097	3.2328	3.1045	2.6463
		10	4.2814	4.2376	4.1972	4.1286	3.8695	2.8498	2.8165	2.7820	2.7181	2.4594
	0.5	0	5.7682	5.3566	5.1043	4.8043	4.1476	3.5060	3.3110	3.1859	3.0237	2.5886
		0.5	5.3395	5.0518	4.8698	4.6429	4.0961	3.3045	3.1668	3.0728	2.9429	2.5618
		1	5.0640	4.8499	4.7090	4.5262	4.0526	3.1684	3.0656	2.9906	2.8814	2.5384
		2	4.7349	4.5966	4.4997	4.3665	3.9852	2.9980	2.9307	2.8765	2.7913	2.4998
		10	4.0677	4.0320	4.0015	3.9522	3.7714	2.6143	2.5896	2.5657	2.5238	2.3595
	1	0	5.1950	4.9013	4.7234	4.5113	4.0290	3.1586	3.0163	2.9261	2.8106	2.4979
		0.5	4.8894	4.6836	4.5543	4.3925	3.9876	3.0130	2.9114	2.8432	2.7504	2.4759
		1	4.6963	4.5411	4.4396	4.3076	3.9533	2.9158	2.8384	2.7834	2.7048	2.4568
		2	4.4641	4.3609	4.2893	4.1908	3.9003	2.7924	2.7401	2.6996	2.6377	2.4254
		10	3.9664	3.9369	3.9123	3.8728	3.7269	2.5011	2.4817	2.4637	2.4329	2.3114
	2	0	4.7064	4.5274	4.4153	4.2774	3.9350	2.8659	2.7752	2.7158	2.6390	2.4216
		0.5	4.5202	4.3911	4.3071	4.1985	3.9034	2.7747	2.7071	2.6609	2.5980	2.4046
		1	4.3997	4.2995	4.2318	4.1408	3.8773	2.7115	2.6582	2.6202	2.5662	2.3897
		2	4.2489	4.1791	4.1291	4.0584	3.8358	2.6276	2.5901	2.5614	2.5182	2.3651
		10	3.8885	3.8650	3.8453	3.8135	3.6931	2.4141	2.3996	2.3865	2.3643	2.2738
	10	0	4.2549	4.1481	4.0789	3.9927	3.7758	2.6079	2.5493	2.5104	2.4600	2.3198
		0.5	4.1470	4.0666	4.0134	3.9442	3.7553	2.5489	2.5035	2.4728	2.4315	2.3069
		1	4.0745	4.0103	3.9667	3.9079	3.7379	2.5068	2.4703	2.4449	2.4093	2.2960
		2	3.9809	3.9345	3.9015	3.8551	3.7102	2.4504	2.4242	2.4049	2.3763	2.2782
		10	3.7486	3.7315	3.7177	3.6958	3.6159	2.3074	2.2971	2.2883	2.2735	2.2156
2	0	0	8.0093	7.2025	6.7083	6.1475	5.0388	4.6592	4.2894	4.0660	3.7955	3.0983
		0.5	7.1630	6.5992	6.2537	5.8474	4.9605	4.2669	4.0174	3.8598	3.6549	3.0586
		1	6.5969	6.1961	5.9428	5.6327	4.8939	3.9984	3.8276	3.7117	3.5492	3.0238
		2	5.9512	5.7154	5.5578	5.3518	4.7918	3.6848	3.5902	3.5169	3.4009	2.9663
		10	4.8391	4.7996	4.7658	4.7100	4.4849	3.0962	3.0729	3.0471	2.9960	2.7580
	0.5	0	6.7530	6.2062	5.8874	5.5302	4.8095	3.9374	3.6777	3.5269	3.3494	2.9074
		0.5	6.1811	5.8067	5.5849	5.3261	4.7492	3.6658	3.4916	3.3852	3.2512	2.8754
		1	5.8216	5.5514	5.3860	5.1857	4.7005	3.4895	3.3668	3.2869	3.1795	2.8481
		2	5.4129	5.2475	5.1406	5.0032	4.6272	3.2829	3.2102	3.1574	3.0791	2.8040
		10	4.6666	4.6335	4.6069	4.5648	4.4010	2.8673	2.8486	2.8302	2.7964	2.6473
	1	0	6.0661	5.6867	5.4688	5.2223	4.6981	3.5421	3.3552	3.2473	3.1211	2.8056
		0.5	5.6689	5.4101	5.2572	5.0762	4.6499	3.3491	3.2223	3.1454	3.0493	2.7797
		1	5.4245	5.2349	5.1189	4.9761	4.6113	3.2254	3.1338	3.0749	2.9969	2.7577
		2	5.1426	5.0226	4.9449	4.8435	4.5527	3.0772	3.0204	2.9803	2.9225	2.7221
		10	4.5863	4.5586	4.5365	4.5014	4.3640	2.7591	2.7438	2.7296	2.7045	2.5947
	2	0	5.4808	5.2614	5.1301	4.9750	4.6073	3.2092	3.0924	3.0216	2.9373	2.7193
		0.5	5.2499	5.0958	5.0003	4.8815	4.5710	3.0910	3.0078	2.9554	2.8894	2.6998
		1	5.1039	4.9873	4.9122	4.8149	4.5413	3.0122	2.9492	2.9079	2.8533	2.6829
		2	4.9265	4.8483	4.7950	4.7218	4.4946	2.9121	2.8708	2.8416	2.8001	2.6551
		10	4.5239	4.5015	4.4830	4.4532	4.3349	2.6768	2.6648	2.6540	2.6354	2.5535

h_{max}/h_{min}	n_z	n_y	$a/b = 1$					$b/a = 2$				
			n_x					n_x				
			0	0.5	1	2	10	0	0.5	1	2	10
	10	0	4.9410	4.8184	4.7410	4.6480	4.4251	2.9159	2.8419	2.7955	2.7403	2.6018
		0.5	4.8174	4.7264	4.6679	4.5946	4.4023	2.8427	2.7871	2.7520	2.7084	2.5878
		1	4.7352	4.6636	4.6163	4.5549	4.3830	2.7921	2.7486	2.7205	2.6842	2.5759
		2	4.6305	4.5799	4.5450	4.4974	4.3521	2.7267	2.6970	2.6767	2.6489	2.5566
		10	4.3775	4.3603	4.3467	4.3256	4.2470	2.5717	2.5622	2.5544	2.5416	2.4889

Table 8. Nondimensional fundamental natural frequency results of CCCC rectangular MFGM plates ($h_{min} = a/10, a = 1$ m)

h_{max}/h_{min}	n_z	n_y	$a/b = 1$					$b/a = 2$				
			n_x					n_x				
			0	0.5	1	2	10	0	0.5	1	2	10
1.5	0	0	11.7926	10.5669	9.8396	9.1461	7.8910	9.0481	7.6178	6.8079	6.1537	5.3995
		0.5	10.8682	9.6664	8.9786	8.3599	7.3582	8.7706	7.3918	6.6204	6.0051	5.3208
		1	10.3207	9.1624	8.5155	7.9549	7.1092	8.5295	7.2169	6.4875	5.9087	5.2775
		2	9.7345	8.6626	8.0806	7.5947	6.9108	8.1233	6.9531	6.3008	5.7826	5.2259
		10	8.4028	7.6397	7.2516	6.9487	6.5732	6.6794	6.0632	5.6857	5.3711	5.0348
	0.5	0	10.0519	9.2140	8.7409	8.2702	7.3682	7.6850	6.7256	6.2211	5.7939	5.2442
		0.5	9.3885	8.5848	8.1476	7.7338	7.0113	7.4823	6.5656	6.0884	5.6886	5.1880
		1	9.0080	8.2430	7.8363	7.4627	6.8454	7.3141	6.4450	5.9948	5.6192	5.1554
		2	8.5984	7.8986	7.5359	7.2126	6.7057	7.0429	6.2648	5.8613	5.5246	5.1133
		10	7.6572	7.1748	6.9384	6.7391	6.4532	6.0968	5.6532	5.4118	5.2054	4.9549
	1	0	9.0746	8.4797	8.1426	7.7951	7.1026	6.9301	6.2586	5.9074	5.5968	5.1650
		0.5	8.5846	8.0208	7.7116	7.4056	6.8410	6.7812	6.1412	5.8091	5.5179	5.1213
		1	8.3030	7.7688	7.4816	7.2045	6.7157	6.6600	6.0524	5.7384	5.4640	5.0945
		2	7.9981	7.5105	7.2541	7.0131	6.6065	6.4675	5.9187	5.6352	5.3880	5.0581
		10	7.2873	6.9509	6.7824	6.6325	6.3976	5.7787	5.4492	5.2745	5.1207	4.9175
	2	0	8.2074	7.8371	7.6153	7.3778	6.8799	6.2717	5.8608	5.6335	5.4222	5.1019
		0.5	7.8863	7.5363	7.3317	7.1192	6.6997	6.1765	5.7828	5.5664	5.3668	5.0685
		1	7.6951	7.3628	7.1719	6.9778	6.6086	6.0982	5.7215	5.5154	5.3261	5.0462
		2	7.4872	7.1814	7.0093	6.8389	6.5266	5.9729	5.6265	5.4381	5.2661	5.0145
		10	6.9837	6.7650	6.6485	6.5400	6.3548	5.4965	5.2745	5.1537	5.0442	4.8875
	10	0	7.2393	7.0423	6.9264	6.8052	6.5414	5.5636	5.3432	5.2239	5.1177	4.9560
		0.5	7.0636	6.8778	6.7716	6.6640	6.4433	5.5063	5.2942	5.1809	5.0809	4.9319
		1	6.9621	6.7859	6.6872	6.5895	6.3956	5.4599	5.2562	5.1483	5.0538	4.9152
		2	6.8525	6.6902	6.6017	6.5163	6.3516	5.3871	5.1984	5.0997	5.0141	4.8905
		10	6.5662	6.4514	6.3928	6.3397	6.2416	5.1178	4.9916	4.9272	4.8723	4.7962
2	0	0	13.9236	12.4359	11.4959	10.5844	9.0515	11.3840	9.6831	8.6369	7.7319	6.6917
		0.5	12.9875	11.5278	10.6326	9.8030	8.5419	11.0574	9.4220	8.4271	7.5727	6.6152
		1	12.4031	10.9954	10.1496	9.3872	8.2993	10.7472	9.2018	8.2653	7.4613	6.5701
		2	11.7339	10.4307	9.6660	8.9951	8.0960	10.1790	8.8425	8.0198	7.3035	6.5113
		10	10.1165	9.1925	8.6788	8.2463	7.7246	8.1709	7.5928	7.1725	6.7632	6.2848
	0.5	0	11.7979	10.8141	10.2363	9.6502	8.5607	9.5963	8.4898	7.8722	7.3153	6.5665
		0.5	11.1274	10.1839	9.6469	9.1229	8.2215	9.3606	8.3069	7.7240	7.2014	6.5105
		1	10.7238	9.8260	9.3247	8.8463	8.0595	9.1505	8.1583	7.6107	7.1197	6.4750
		2	10.2616	9.4412	8.9926	8.5739	7.9147	8.7901	7.9214	7.4371	6.9993	6.4249
		10	9.1308	8.5694	8.2759	8.0117	7.6248	7.5265	7.0915	6.8256	6.5705	6.2243

h_{max}/h_{min}	n_z	n_y	$a/b = 1$					$b/a = 2$				
			n_x					n_x				
			0	0.5	1	2	10	0	0.5	1	2	10
		0	10.6283	9.9532	9.5593	9.1425	8.3096	8.6279	7.8787	7.4682	7.0814	6.4993
		0.5	10.1359	9.4967	9.1339	8.7620	8.0615	8.4569	7.7456	7.3583	6.9950	6.4547
	1	1	9.8400	9.2350	8.8972	8.5573	7.9386	8.3091	7.6379	7.2730	6.9308	6.4243
		2	9.4998	8.9487	8.6465	8.3482	7.8238	8.0616	7.4654	7.1396	6.8328	6.3793
		10	8.6527	8.2764	8.0775	7.8886	7.5761	7.1638	6.8388	6.6512	6.4686	6.1936
		0	9.6031	9.2060	8.9613	8.6875	8.0920	7.7932	7.3610	7.1121	6.8627	6.4386
		0.5	9.2845	8.9099	8.6836	8.4362	7.9211	7.6861	7.2736	7.0370	6.8009	6.4030
	2	1	9.0869	8.7317	8.5200	8.2922	7.8311	7.5934	7.2004	6.9756	6.7517	6.3767
		2	8.8587	8.5323	8.3411	8.1394	7.7432	7.4378	7.0804	6.8762	6.6733	6.3357
		10	8.2647	8.0332	7.9031	7.7726	7.5323	6.8328	6.6185	6.4940	6.3692	6.1628
		0	8.4687	8.2636	8.1365	7.9971	7.7026	6.9091	6.6864	6.5574	6.4324	6.2353
		0.5	8.2980	8.1043	7.9872	7.8620	7.6103	6.8465	6.6324	6.5098	6.3918	6.2088
	10	1	8.1944	8.0105	7.9012	7.7865	7.5627	6.7934	6.5880	6.4714	6.3598	6.1887
		2	8.0751	7.9055	7.8069	7.7058	7.5142	6.7066	6.5174	6.4111	6.3100	6.1573
		10	7.7425	7.6222	7.5564	7.4924	7.3781	6.3821	6.2593	6.1916	6.1278	6.0344

Table 9. Nondimensional fundamental natural frequency results of circular MFGM plates ($h_{min} = R/10, R = 1$ m)

BCs	h_{max}/h_{min}	n_z	n_r				
			0	0.5	1	2	10
Sr	1.5	0	6.8608	6.0005	5.3686	4.6140	3.6240
		0.5	5.5290	4.9722	4.5859	4.1401	3.5663
		1	4.9383	4.5216	4.2462	3.9366	3.5419
		2	4.5096	4.1990	4.0056	3.7943	3.5255
		10	4.0947	3.9060	3.7934	3.6711	3.5113
	2	0	9.1898	7.8911	6.9925	6.0121	4.8314
		0.5	7.2028	6.4315	5.9269	5.3906	4.7556
		1	6.2788	5.7707	5.4508	5.1156	4.7230
		2	5.5947	5.2910	5.1093	4.9217	4.7013
		10	5.1486	4.9956	4.9064	4.8115	4.6900
	4	0	18.4511	14.9260	12.9486	11.2748	9.6062
		0.5	14.2902	12.2383	11.1801	10.3164	9.4858
		1	12.2349	10.9744	10.3571	9.8705	9.4319
		2	10.5930	10.0111	9.7431	9.5474	9.3966
		10	9.6830	9.5503	9.4907	9.4413	9.3895
Cr	1.5	0	11.5326	8.9995	7.9595	7.1588	6.0711
		0.5	9.7728	7.9378	7.2122	6.6723	5.9912
		1	8.8030	7.4152	6.8628	6.4575	5.9585
		2	7.9778	7.0098	6.6048	6.3073	5.9371
		10	7.2090	6.5827	6.3355	6.1513	5.9115
	2	0	13.3562	10.5371	9.3212	8.3290	7.0203
		0.5	11.2485	9.1737	8.3293	7.6879	6.9205
		1	10.1012	8.5045	7.8648	7.4020	6.8790
		2	9.1212	7.9815	7.5204	7.2022	6.8524
		10	8.2088	7.4926	7.2318	7.0505	6.8314

BCs	h_{max}/h_{min}	n_z	n_r				
			0	0.5	1	2	10
	4	0	21.2649	16.9794	14.8115	13.0147	11.1031
		0.5	17.4714	14.3756	12.9841	11.9539	10.9544
		1	15.5088	13.1266	12.1358	11.4689	10.8898
		2	13.8368	12.1448	11.5033	11.1271	10.8491
		10	12.3303	11.4239	11.1465	10.9870	10.8367

4. Conclusions

In this study, the static linear bending and free vibration analyses of MFGM plates with variable thickness are conducted. The governing equations of the problems are derived based on the third-order shear deformation plate theory and Hamilton's principle. The material constituents of MFGM are assumed to change spatially within the plates' volume. The IGA approach is then used as a discretization tool to solve the governing equations of the problems, where NURBS basis functions are adopted to model the geometries of the plate and interpolate the displacement variables. Various numerical examples are carried out to validate the accuracy of the proposed approach and investigate the influence of geometrical and material parameters. The results obtained from this study could be used as benchmark solutions for further investigation of MFGM plates with variable thickness.

Acknowledgements

This research is funded by Vietnam National University Ho Chi Minh City under grand number C2021-20-35. We acknowledge the support of time and facilities from Ho Chi Minh City University of Technology (HCMUT), VNU-HCM for this study.

References

[1] Oscar Barton, J. (1999). Fundamental frequency of tapered plates by the method of eigensensitivity analysis. *Ocean Engineering*, 26(6):565–573.

[2] Ahari, M. N., Eshghi, S., Ashtiany, M. G. (2009). The tapered beam model for bottom plate uplift analysis of unanchored cylindrical steel storage tanks. *Engineering Structures*, 31(3):623–632.

[3] Susantha, K. A. S., Aoki, T., Kumano, T. (2006). Strength and ductility evaluation of steel bridge piers with linearly tapered plates. *Journal of Constructional Steel Research*, 62(9):906–916.

[4] Bowyer, E. P., O'Boy, D. J., Krylov, V. V., Gautier, F. (2013). Experimental investigation of damping flexural vibrations in plates containing tapered indentations of power-law profile. *Applied Acoustics*, 74 (4):553–560.

[5] Leissa, A. W. (1969). *Vibration of plates*. Scientific and Technical Information Division, National Aeronautics and Space Administration.

[6] Tweet, K. D., Forrestal, M. J., Baker, W. E. (1997). Diverging elastic waves in thin tapered plates. *International Journal of Solids and Structures*, 34(3):289–296.

[7] Cheung, Y. K., Ding, Z. (1999). Eigenfrequencies of tapered rectangular plates with intermediate line supports. *International Journal of Solids and Structures*, 36(1):143–166.

[8] Lotfi, S., Azhari, M., Heidarpour, A. (2011). Inelastic initial local buckling of skew thin thickness-tapered plates with and without intermediate supports using the isoparametric spline finite strip method. *Thin-Walled Structures*, 49(11):1475–1482.

[9] Cheung, Y. K., Zhou, D. (2003). Vibration of tapered Mindlin plates in terms of static Timoshenko beam functions. *Journal of Sound and Vibration*, 260(4):693–709.

[10] Wang, F., fang Zheng, Y., ping Chen, C. (2018). Nonlinear bending of rectangular magnetoelectroelastic thin plates with linearly varying thickness. *International Journal of Nonlinear Sciences and Numerical Simulation*, 19(3-4):351–356.
[11] Wang, C. M. (1997). Relationships between Mindlin and Kirchhoff bending solutions for tapered circular and annular plates. *Engineering Structures*, 19(3):255–258.
[12] Wang, C. M., Hong, G. M., Tan, T. J. (1995). Elastic buckling of tapered circular plates. *Computers & Structures*, 55(6):1055–1061.
[13] Zenkour, A. M. (2018). Bending of thin rectangular plates with variable-thickness in a hygrothermal environment. *Thin-Walled Structures*, 123:333–340.
[14] Ansari, E., Setoodeh, A. (2020). Applying isogeometric approach for free vibration, mechanical, and thermal buckling analyses of functionally graded variable-thickness blades. *Journal of Vibration and Control*, 26(23-24):2193–2209.
[15] Koizumu, M. (1993). The concept of FGM, ceramic transactions. *Functionally Graded Materials*, 34: 3–10.
[16] Thai, H.-T., Kim, S.-E. (2015). A review of theories for the modeling and analysis of functionally graded plates and shells. *Composite Structures*, 128:70–86.
[17] Jha, D. K., Kant, T., Singh, R. K. (2013). A critical review of recent research on functionally graded plates. *Composite Structures*, 96:833–849.
[18] Swaminathan, K., Naveenkumar, D. T., Zenkour, A. M., Carrera, E. (2015). Stress, vibration and buckling analyses of FGM plates—A state-of-the-art review. *Composite Structures*, 120:10–31.
[19] Tran, T. T., Pham, Q.-H., Nguyen-Thoi, T. (2021). Static and free vibration analyses of functionally graded porous variable-thickness plates using an edge-based smoothed finite element method. *Defence Technology*, 17(3):971–986.
[20] Van Vinh, P. (2021). Formulation of a new mixed four-node quadrilateral element for static bending analysis of variable thickness functionally graded material plates. *Mathematical Problems in Engineering*, 2021.
[21] Lal, R., Saini, R. (2020). Vibration analysis of FGM circular plates under non-linear temperature variation using generalized differential quadrature rule. *Applied Acoustics*, 158:107027.
[22] Kumar, V., Singh, S. J., Saran, V. H., Harsha, S. P. (2020). An analytical framework for rectangular FGM tapered plate resting on the elastic foundation. *Materials Today: Proceedings*, 28:1719–1726.
[23] Kumar, V., Singh, S. J., Saran, V. H., Harsha, S. P. (2021). Vibration characteristics of porous FGM plate with variable thickness resting on Pasternak's foundation. *European Journal of Mechanics - A/Solids*, 85: 104124.
[24] Kumar, V., Singh, S. J., Saran, V. H., Harsha, S. P. (2020). Exact solution for free vibration analysis of linearly varying thickness FGM plate using Galerkin-Vlasov's method. *Proceedings of the Institution of Mechanical Engineers, Part L: Journal of Materials: Design and Applications*, 235(4):880–897.
[25] Minh, P. P., Manh, D. T., Duc, N. D. (2021). Free vibration of cracked FGM plates with variable thickness resting on elastic foundations. *Thin-Walled Structures*, 161:107425.
[26] Hosseini-Hashemi, S., Taher, H. R. D., Akhavan, H. (2010). Vibration analysis of radially FGM sectorial plates of variable thickness on elastic foundations. *Composite Structures*, 92(7):1734–1743.
[27] Ghatage, P. S., Kar, V. R., Sudhagar, P. E. (2020). On the numerical modelling and analysis of multi-directional functionally graded composite structures: A review. *Composite Structures*, 236:111837.
[28] Nemat-Alla, M. (2003). Reduction of thermal stresses by developing two-dimensional functionally graded materials. *International Journal of Solids and Structures*, 40(26):7339–7356.
[29] Lieu, Q. X., Lee, S., Kang, J., Lee, J. (2018). Bending and free vibration analyses of in-plane bi-directional functionally graded plates with variable thickness using isogeometric analysis. *Composite Structures*, 192: 434–451.
[30] Lieu, Q. X., Lee, J. (2019). A reliability-based optimization approach for material and thickness composition of multidirectional functionally graded plates. *Composites Part B: Engineering*, 164:599–611.
[31] Alipour, M. M., Shariyat, M., Shaban, M. (2010). A semi-analytical solution for free vibration of variable thickness two-directional-functionally graded plates on elastic foundations. *International Journal of*

Mechanics and Materials in Design, 6(4):293–304.

[32] Shariyat, M., Alipour, M. M. (2013). A power series solution for vibration and complex modal stress analyses of variable thickness viscoelastic two-directional FGM circular plates on elastic foundations. *Applied Mathematical Modelling*, 37(5):3063–3076.

[33] Thai, S., Nguyen, V. X., Lieu, Q. X. (2022). Bending and free vibration analyses of multi-directional functionally graded plates in thermal environment: A three-dimensional Isogeometric Analysis approach. *Composite Structures*, 295:115797.

[34] Temel, B., Noori, A. R. (2020). A unified solution for the vibration analysis of two-directional functionally graded axisymmetric Mindlin–Reissner plates with variable thickness. *International Journal of Mechanical Sciences*, 174:105471.

[35] Zhong, S., Jin, G., Ye, T., Zhang, J., Xue, Y., Chen, M. (2020). Isogeometric vibration analysis of multi-directional functionally gradient circular, elliptical and sector plates with variable thickness. *Composite Structures*, 250:112470.

[36] Jalali, S. K., Heshmati, M. (2020). Vibration analysis of tapered circular poroelastic plates with radially graded porosity using pseudo-spectral method. *Mechanics of Materials*, 140:103240.

[37] Reddy, J. N. (1984). A simple higher-order theory for laminated composite plates. *Journal of Applied Mechanics*, 51(4):745–752.

[38] Hughes, T. J. R., Cottrell, J. A., Bazilevs, Y. (2005). Isogeometric analysis: CAD, finite elements, NURBS, exact geometry and mesh refinement. *Computer Methods in Applied Mechanics and Engineering*, 194(39-41):4135–4195.

[39] Nguyen, V. P., Anitescu, C., Bordas, S. P. A., Rabczuk, T. (2015). Isogeometric analysis: An overview and computer implementation aspects. *Mathematics and Computers in Simulation*, 117:89–116.

[40] Shufrin, I., Eisenberger, M. (2006). Vibration of shear deformable plates with variable thickness — first-order and higher-order analyses. *Journal of Sound and Vibration*, 290(1-2):465–489.

[41] Mlzusawa, T. (1993). Vibration of rectangular mindlin plates with tapered thickness by the spline strip method. *Computers & Structures*, 46(3):451–463.

[42] Bacciocchi, M., Eisenberger, M., Fantuzzi, N., Tornabene, F., Viola, E. (2016). Vibration analysis of variable thickness plates and shells by the Generalized Differential Quadrature method. *Composite Structures*, 156:218–237.

[43] Son, T., Huu-Tai, T. (2019). Free-vibration analysis of multi-directional functionally graded plates based on 3D isogeometric analysis. *Journal of Science and Technology in Civil Engineering (STCE) - HUCE*, 13(2):1–11.